EAST EUROPEAN JOURNAL OF PHYSICS. **2.** 282-288 (2023)
DOI:10.26565/2312-4334-2023-2-32 ISSN 2312-4334

THE EFFECT OF DIFFUSENESS PARAMETER ON THE QUASI-ELASTIC SCATTERING OF THE $^{25}Mg + {}^{90}Zr$ and $^{28}Si + (^{120}Sn, {}^{150}Nd)$ SYSTEMS USING WOOD-SAXON POTENTIAL[†]

Farah J. Hamood[§], Khalid S. Jassim*
Department of Physics, College of Education for pure Sciences, University of Babylon, Iraq.
[§]E-mail: pure.farah.jabar@uobabylon.edu.iq
Corresponding Author e-mail: khalidsj@uobabylon.edu.iq
Received march 12, 2023; revised April 30, 2023; accepted May 2, 2023

In this research, the effect of changing the values of the diffusion parameter on the semi-elastic scattering ($\frac{d\sigma qel}{d\sigma R}$) and distribution (D) calculations for single channel (SC) and coupled channel (CC) have been studied. Three values were taken from the diffusion for each system parameter. It is assumed that the nuclear potential has a Woods-Saxon form, which is indicated by the surface diffuseness, potential depth, and radius parameters for ($^{25}Mg + {}^{90}Zr$), ($^{28}Si + (^{120}Sn, {}^{150}Nd)$ Systems. The chi square (χ^2) is applied to compare the best fitted value of the diffuseness parameter between the theoretical calculations and the experimental data. According to the results of (χ^2), we noticed that some systems achieved a good match between the theoretical calculations and experimental data of semi-elastic scattering ($\frac{d\sigma qel}{d\sigma R}$) and the distribution calculations at the standard value of the diffusion parameter (a_0=0.63) or at a value higher and lower than the standard value .In the case of channel is single SC the best fit was at a value less than the standard value of the diffusivity parameter, but in the case of CC the fit was better at a value higher than the standard value of the surface diffuseness parameter because the potential barrier in the single SC, while in CC calculations it is multiple.
Keywords: *Quasi-elastic scattering; Woods-Saxon potential; Single channel; Coupled channels; Surface diffuseness parameter; Heavy-ion system*
PACS: 21.60.-n, 21.10.-k, 21.60.Jz, 25.70.Bc, 25.70.

1. INTRODUCTION

The Nuclear reactions at sub-barrier energy are crucial in nature, since they are responsible for the basic behavior of stars, their development, and many aspects of element production. The nucleus potential is consist from Coulomb $V_C(r)$ and nuclear $V_N(r)$ parts [1][2]. The Woods-Saxon (WS) form is often used to represent the nuclear component, which is characterized by the deepness V_0, radius r_0, and diffuseness a_0 parameters. It is significant in nuclear physics because it is regarded as a realistic potential [3]. Experiments indicate that coupling to collective states results in a distribution of Coulomb barrier heights, which may be calculated directly from the fusion excitation function σ_{fus} (E) or from back scattered quasi elastic events for many nuclear systems. A significant method for the investigation of barrier distributions near to the Coulomb barrier is large back-angle quasi elastic scattering [4]. It may be described as the total of elastic scattering, inelastic scattering, and transfer reaction. It is very similar to the fusion process which is defined as a reaction in which two discrete nuclei combine to produce a compound system [5]. Heavy-ion collisions at energies around the Coulomb barrier are strongly affected by the internal structure of colliding nuclei [6]. The coupling channel model is the best instrument for simultaneously reproducing the experimental data for a variety of events, including particle transfers, fusion, elastic and inelastic scattering [7]. The inter-nuclear potential is the most crucial factor in calculations involving coupled channels. Since it has an impact on the coupling strengths and the breadth of the barrier. The transfer reactions, as well as the collective vibrational and rotational movements, are coupled with the relative motion of the colliding nuclei to produce the channel coupling [8]. A heavy-ion reaction to fusion has a counterpart in quasi-elastic heavy-ion scattering at reverse angles. At energies near to the Coulomb barrier, these inclusive procedures are vulnerable to channel coupling effects (due to collective inelastic excitations of the colliding nuclei). The likelihood of reflection at the Coulomb barrier causes quasi-elastic scattering, whereas transmission is connected to fusion. This fact was exploited, and barrier distributions were obtained [9]. Fusion is one of the most significant near-barrier processes. The interaction between the relative velocity of two colliding nuclei and their internal structures is well known to result in a significant increase in fusion cross sections at sub-barrier energy [1]. Several studies on quasi elastic scattering have been studied by Khalid S. Jassim for some heavy ions systems [10-12].

The aim of this research study is to study quasi elastic scattering at near energies from high the coulomb potential barrier to determine the surface diffuseness parameters of the inter-nucleus potential for the systems $^{25}Mg+{}^{90}Zr$ and $(^{28}Si, {}^{120}Sn)+{}^{150}Nd$ single and coupled channels calculations were performed using the CQEL program [7], which includes all orders of coupling and is the most recent iteration of the computer code CCFULL. The chi square (χ^2) approach has been used to find the diffuseness parameters' best fitted values in comparison to the experimental data.

[†] ***Cite as:*** F.J. Hamood, and K.S. Jassim, East Eur. J. Phys. **2**, 282 (2023), https://doi.org/10.26565/2312-4334-2023-2-32

2. THEORY

The potential between two nuclei consists of two parts, the first part being the nuclear potential Vn, which may be adequately and reasonably characterized by the two parts that make up the nucleus-nucleus potential. The Woods-Saxon (WS) form provided by [12].

$$V_N(r) = -\frac{V_\circ}{1+e^{\left[\frac{r-R_\circ}{a}\right]}}, \tag{1}$$

where r is the center-of-mass separation between the target nucleus of mass number A_T and the projectile nucleus of mass number A_P, and R_0 denotes the system's radius $R_0 = r_0\left(A_T^{\frac{1}{3}} + A_P^{\frac{1}{3}}\right)$. When they do not interact, the second part being the Coulomb potential V_C between two spherical nuclei with uniform charge density distributions is given by [12]:

$$V_c(r) = \frac{Z_P Z_T\ e^2}{r}, \tag{2}$$

here **r** is the distance between the centers of mass of the colliding nuclei and Z_p and Z_T are the atomic numbers of the projectile and target, respectively.

The Coulomb potential is produced when the nuclei interact, and it is determined by[13].

$$V_c(r) = \frac{Z_P Z_T\ e^2}{2R_C}\left[3 - \left(\frac{r}{R_c}\right)^2\right], \tag{3}$$

where R_c is the radius of the equivalent sphere, which corresponds to the projectile and target nuclei.

The coupling between the nuclear intrinsic motion and the relative motion of the centers of mass of the colliding nuclei, r = (r, r), which causes the collision of two nuclei. The Hamiltonian system's is provided by [4] :

$$H(\vec{r}.\xi) = -\frac{\hbar^2}{2\mu}\nabla^2 + V(r) + H_0(\xi) + V_{coup}(\vec{r}.\xi), \tag{4}$$

where V (r) is the bare potential in the absence of coupling where V(r)= V N (r)+V c (r) , $H_0(\xi)$ is the Hamiltonian for the intrinsic motion, and Ccoup is the stated coupling, r stands for the center of mass distance between the colliding nuclei.

The entire wave function's Schrodinger equation is given by[14].

$$\left(-\frac{\hbar^2}{2\mu}\nabla^2 + \mathrm{V(r)} + \mathrm{H_0(\xi)} + \mathrm{V_{coup}}(\vec{\mathrm{r}}.\xi)\right)\psi(\vec{\mathrm{r}}.\xi) = \mathrm{E}\psi(\vec{\mathrm{r}}.\xi), \tag{5}$$

Generally, the internal degree of freedom has a limited spin. The coupling Hamiltonian in complexities can be written as [4] :

$$V_{coup}(\vec{r}.\xi) = \sum_{\lambda>0.\mu} f_\lambda\ (r) Y_{\lambda\mu}(\hat{\mathrm{r}}).\mathrm{T}_{\lambda\mu}(\xi), \tag{6}$$

The spherical harmonics and spherical tensors, which are constructed from the internal coordinate, are denoted by $Y_{\lambda\mu}(\hat{\mathrm{r}})$ and $\mathrm{T}_{\lambda\mu}(\xi)$, respectively. That when it was taken into account in V (r), the total is taken over all values of excluding for λ = 0. (r). For a constant total angular momentum J and its z-component M, the expansion basis for the wave function in Eq. (5) is given by [4] :

$$\langle \vec{r}\,\xi|(nlI)JM\rangle = \sum_{m_1 m_I}\langle l m_l\, I m_I|JM\rangle Y_{lm_l}(\hat{\mathrm{r}})\,\varphi_{nIm_I}(\xi), \tag{7}$$

where in *l* denotes the orbital, I denotes internal angular momenta, and $\varphi_{nIm_I}(\xi)$ denotes the wave function for the internal motion that which fulfills by equation below[4] :

$$H_0(\xi)\,\varphi_{nIm_I}(\xi) = \epsilon_n\,\varphi_{nIm_I}(\xi)\,, \tag{8}$$

With this basis, the total wave function $\psi(\vec{r}.\xi)$has been expansion as [15]:

$$\psi(\vec{r}.\xi) = \sum_{n.l.I}\frac{u^J_{nlI}(r)}{r}\langle \vec{r}\,\xi|(nlI)JM\rangle, \tag{9}$$

It is possible to write the Schrödinger equation [Eq. (3)] as a group of coupled equations for $u^J_{nlI}(r)$ [14] :

$$\left[-\frac{\hbar^2}{2\mu}\frac{d^2}{dr^2} + V(r) + \frac{l(l+1)\hbar^2}{2\mu r^2} - E + \epsilon_n\right]u^J_{nlI}(r) + \sum_{\acute{n}.l'.\acute{I}} V^J_{nlJ;\acute{n}.l'.\acute{I}}(r)u^J_{\acute{n}.l'.\acute{I}}(r) = 0, \tag{10}$$

The coupling matrix elements $V^J_{nlJ;\acute{n}.l'.\acute{I}}(r)$, According to [4] are as follows:

$$V^J_{nlJ;\acute{n}.\acute{l}.\acute{I}}(r) = \langle JM\,(nlI)\left|V_{coup}(\vec{r}.\xi)\right|\left(\acute{n}.l'.\acute{I}\right)JM\rangle = \sum_\lambda(-1)^{I-\acute{I}+l'+J} f_\lambda(r)\langle l||Y_\lambda||l'\rangle\langle nI||T_\lambda||n'I'\rangle \times \sqrt{(2l+1)(2I+1)}\begin{Bmatrix} I' & l' & J \\ l & I & \lambda\end{Bmatrix}, \tag{11}$$

Where the reduced matrix elements in Eq. (8) is defined as follows [4]:

$$\langle l_{ml}|Y_{\lambda\mu}|l'_{ml'}\rangle = \langle l'_{ml'}\,\lambda\mu|l_{ml}\rangle\,\langle l||Y_{\lambda}||l'\rangle, \tag{12}$$

where $V^{J}_{nlJ;ń.l'.Ĩ}(r)$ are separate of the index M, the index has been suppressed as seen in Eq. (11). Coupled-channels equations are the name given to the equation (10). For heavy-ion fusion reactions, these equations are usually solved using the incoming wave boundary conditions[14].

$$u^{J}_{nlI}(r) \sim \mathcal{T}^{J}_{nlI}\; exp\left(-1\int_{r_{abs}}^{r} k_{nlI}\,(ŕ)dŕ\right)\; .r \leqslant r_{abs}, \tag{13}$$

$$\frac{i}{2}\left(H_{l}^{(-)}\,(k_{nIr})\delta_{n,n_i}\delta_{l,l_i}\delta_{I,I_i} + \sqrt{\frac{k_{nIi}}{k_{nI}}}\;S^{J}_{ll}H_{l}^{(+)}(k_{nIr})\right)\,,r \longrightarrow \infty\,, \tag{14}$$

where $k_{nIr} = \sqrt{2\mu(E-\epsilon_{nI})/\hbar^2}$, $k_{nIi} = k = \sqrt{2\mu E/\hbar^2}$ and the following formula defines the local wave number k_{nII}:

$$k_{nII}(r) = \sqrt{\frac{2\mu}{\hbar^2}\left(E - \epsilon_{nI} - \frac{l(l+1)\hbar^2}{2\mu r^2} - V(r) - V^{J}_{nlJ;nlJ}(r)\right)}, \tag{15}$$

After obtaining the transmission coefficients T nlIJ, the penetrability via the Coulomb barrier is given by:

$$P^{J}_{liIi}(E) = \sum_{n.l.I}\frac{k_{nlI}(r_{abs})}{k}|\mathcal{T}^{J}_{nlI}|^2, \tag{16}$$

The computation of quasi-elastic cross sections typically needs a high value of angular momentum in order to provide convergent results, unlike the calculation of fusion cross sections. For such a huge angular momentum, the potential pocket at (r = rabs) becomes shallow or even vanishes. Therefore, it is impossible to precisely identify the incoming flux in Eq. (13). In order to avoid employing the incoming wave boundary conditions, the quasi-elastic problem often executes the regular boundary conditions at the origin. A complex potential V N (r)= V N_0 (r)+iw(r) is required to model the fusion reaction when utilizing the usual boundary conditions. Following the acquisition of the nuclear S-matrix in Equation (Eq11), the scattering amplitude may be computed as

$$f^{J}_{lI}(\theta.E) = i\sum_{Jl}\sqrt{\frac{\pi}{kk_{nI}}}i^{J-l}\;e^{i[\sigma_J(E)+\sigma_l(E-\epsilon_{nI})]}\sqrt{2J+1}\;Y_{l0}(\theta)\left(S^{J}_{u} - \delta_{I.I_2}\delta_{l.l_2}\right) + f_c(\theta.E)\delta_{I.I_2}\delta_{l.l_2} \tag{17}$$

The Coulomb phase shift is σ_l.and given by the equation,

$$\sigma_l = |\Gamma(l+1+i\eta)|, \tag{18}$$

As for f_c, which is the Coulomb scattering amplitude and is determined by [14]:

$$f_c(\theta.E) = \frac{\eta}{2ksin^2\left(\frac{\theta}{2}\right)}e^{\left[-i\eta ln\left(sin^2\left(\frac{\theta}{2}\right)\right)+2i\sigma_0(E)\right]}, \tag{19}$$

here η = is the Sommerfeld parameter which is given by $\eta = Z_1Z_2\,e^2/\hbar v$, and utilizing Equation (16), the differential cross section may be evaluated

$$\frac{d\sigma_{qel}(\theta.E)}{d\Omega} = \sum_{Jll}\frac{k_{nI}}{k}|f^{J}_{ll}(\theta.E)|^2, \tag{20}$$

may be evaluate the Rutherford cross section.

$$\frac{d\sigma_R(\theta.E)}{d\Omega} = |f_c(\theta.E)|^2 = \frac{\eta^2}{4k^2}csc^4\left(\frac{\theta}{2}\right), \tag{21}$$

The distribution of the barrier of fusion is defined as [4] :

$$D_{fus}(E) = \frac{d^2}{dE^2}\left[E\;\sigma_{fus}(E)\right], \tag{22}$$

The definition of the total scattering distribution of the barrier of scattering D_{tot} (E) is [4]:

$$D_{tot}(E) = -\frac{d}{dE}\left[\frac{d\sigma_{tot}}{d\sigma_R}(E)\right], \tag{23}$$

3. RESULTS AND DISCUSSION

Calculations for single-channel and coupled channels were performed using the CQEL code last version [7], which is thought to be the most recent iteration of the computer code CCFULL . This program precisely resolves the linked equations and the Schrödinger equation. The chi square methods have been used in the present work to prevent systematic mistakes, where the data with dqel /dR>1 were omitted from the fitting procedures. The chi square technique χ^2 was regarded as a normalizing factor between the theoretical calculation and the experimental data. the main potential in this work is Wood-Saxon (WS), which has both real and fictitious components. The fairly tiny internal potential was explained by the fictitious potential. A change has been made to done on the real potential's parameters to determine how best to fit the experimental data, and it was then repeated for all interactions. The value of 0.63 is

considered a constant for the diffuseness parameter [15], and a higher and lower value is taken for each system, It differs from one system to another and the radius parameter is assumed to be r_0 1.2 fm.

4-1. The ^{24}Mg + ^{90}Zr reaction

In this system, the results were processed in two cases, the first case, where both the projectile and target nuclei were considered inert (SC) at different values of the diffusion parameter (0.69, 0.63, and 0.57) fm, respectively and we considered the diffusion parameter 0.63 fm is the standard value. In the second case, the projectile nucleus was ^{24}Mg rotates with a deformation coefficient of $\beta_2 = 0.374$ to the state 2^+ (1.368672 MeV) and this was deduced according to the ratio $E_{4^+}/E_{2^+} = 3.012$ while the target core ^{90}Zr was vibrating with a deformation coefficient of $\beta_2 = 0.089$ to the state 2^+(2.186273 MeV), where $E_{4^+}/E_{2^+} = 1.4$ at coupled-channel (CC). We used the single phonon state of the quadrupole excitation of the projectile and target nuclei, the potential depth V_0 = 58.8 MeV, and the radius parameter r_0 = 1.2 fm.

Table 1. The values of the **WS** potential's parameters and χ^2 fitting between experimental and theoretical data for the **^{24}Mg + ^{90}Zr** reaction.

System	Channel	V_0 (MeV)	r_0 (fm)	a_0 (fm)	θ_{cm} $(deg.)$	χ^2	
						σ_{qel}/σ_R	D_{qel}
^{24}Mg +^{90}Zr	SC	58.8	1.2	0.57	158	0 .28177	0.07342
				0.63		3.47134	0.33499
				0.69		12.68139	0.88261
	CC	58.8	1.2	0.57	158	0.01071	0.04572
				0.63		0.02178	0.02036
				0.69		0.07305	0.02015

From Table (1), it is shown that, according to the results of the χ2, the calculated ratio of the quasi-elastic to the Rutherford cross sections $\left(\frac{d\sigma_{qel}}{d\sigma_R}\right)$ is 0.28177 at the diffuseness parameter 0.57 fm, V_0 = 58.8 MeV, which was obtained from the SC data analysis where the projectile ^{24}Mg nucleus and target ^{90}Zr nucleus are inert and is represented by the hard red line in Fig. 1.a. (A),

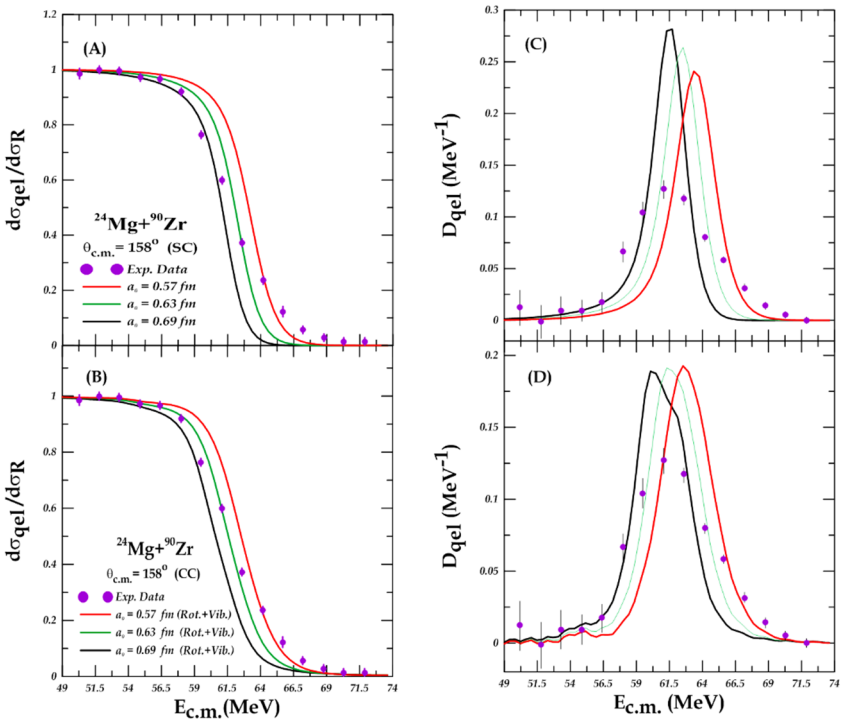

(a) (b)

Figure 1.a. The ratio of the quasi-elastic scattering to the Rutherford cross sections for ^{25}Mg+^{90}Zr system at sub-barrier energies. Banal A and B using the single channel and coupled-channels calculations, respectively. **Figure 1.b.** (C, D) shows the distribution at sub-barrier energies, using the single and coupled channels calculations, respectively. The experimental data are taken from Ref [16].

It is the curve closest to the curve of the experimental data; the best value of the distribution D is 0.33499 at the same value of a_0 which is represented by the black colored. According to the coupled-channel calculation with a rotating projectile (P) and a vibrating target (T), the best value of $\left(\frac{d\sigma_{qel}}{d\sigma_R}\right)$ is 0.01071 at the diffuseness parameter a_0 = 0.57 fm is represented by the hard red line in Fig. 1.b (B). From the Fig. 1.b. (C) the best value of the distribution D is 0.015 at the diffuseness parameter of 0.69 fm, which is represented by the black colored.

4-2. The $^{28}Si+^{120}Sn$ system

From Throughout this system, the findings were processed in two distinct ways. In the first case, we assumed that the diffusion parameter 0.63fm was the standard value and that both the projectile and target nuclei were inert (SC) at various values (0.60, 0.63, and 0.66) fm respectively. In the second instance, the target core ^{120}Sn was vibration with a deformation coefficient of $\beta_2 = 0.107$ to the state 2^+ (1.171265 Mev), $E_{4^+}/E_{2^+} = 1.8$ at coupled-channel (CC), whereas the projectile nucleus was ^{28}Si rotation with a deformation coefficient of β_2 = -0.478 to the state 2^+(1.77903 MeV), where $E_{4^+}/E_{2^+} = 2.59$. The potential depth V_0= 45.8 MeV, the radius parameter r_0 =1.2 fm, and the single phonon state of the quadruple excitation of the projectile and target nuclei were employed.

Table 2. The values of the **WS** potential's parameters and χ^2 fitting between experimental and theoretical data for the $^{28}Si+^{120}Sn$ reaction

System	Channel	V_0 (MeV)	r_0 (fm)	a_0 (fm)	θ_{cm} $(deg.)$	χ^2	
						σ_{qel}/σ_R	D_{qel}
$^{28}Si+^{120}Sn$	SC	45.8	1.2	0.60	150.5	0.06072	0.03304
				0.63		0.10359	0.05258
				0.66		0.17721	0.08379
	CC	45.8	1.2	0.60	150.5	0.01259	0.01686
				0.63		0.00794	0.01954
				0.66		0.00475	0.02127

According to Table (2), the results of χ^2 show that the calculated ratio of the quasi-elastic to the Rutherford cross sections $\left(\frac{d\sigma_{qel}}{d\sigma_R}\right)$ is 0.06072 at the diffuseness parameter of 0.60 fm, which was obtained from single channel (SC) data analysis where the projectile ^{28}Si nucleus and target ^{120}Sn nucleus are inert, and is represented by the hard red line in Fig. 2.a. (A) It is the curve that is closest to the experimental data curve; the best value for the distribution D is 0.03304, which is represented by the hard red line in Fig. 2.b. while the coupled-channel calculations with a rotating projectile (P) and vibrating target (T), it was found that the best value of $\left(\frac{d\sigma_{qel}}{d\sigma_R}\right)$ is 0.00475 at the diffuseness parameter 0.66 fm, which is represented by the solid black line in Fig. 2.b. (B), where V_0 = 45.8 MeV. It is the curve closest to the curve of the experimental data, the best value for the distribution D is 0.01686 at the diffuseness parameter 0.60 fm denoted by the red-colored curve.

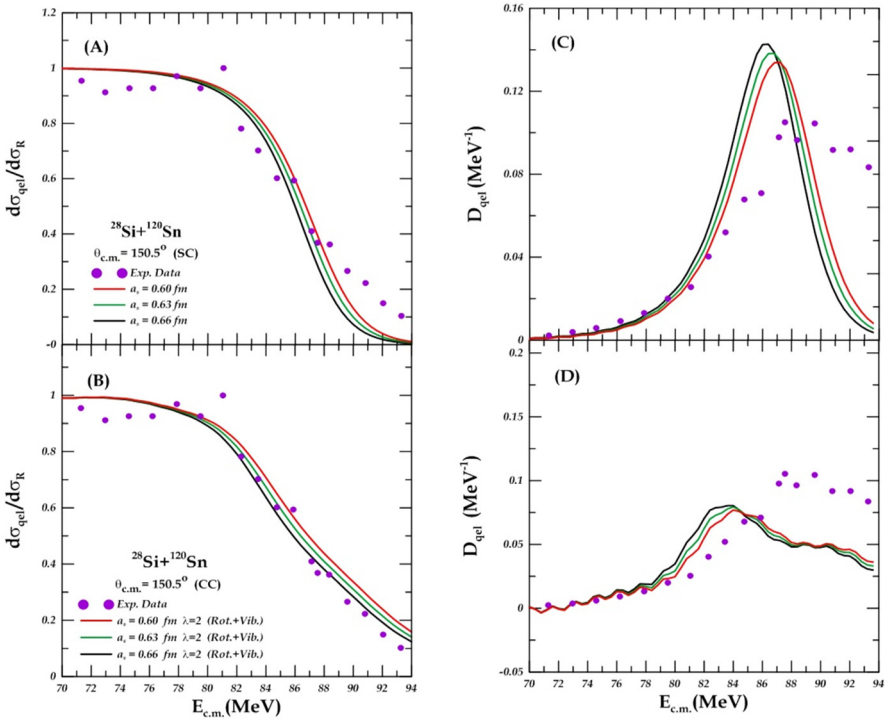

(a) (b)

Figure 2.a. The ratio of the quasi-elastic scattering to the Rutherford cross sections for $^{28}Si+^{120}Sn$ system at sub-barrier energies. Banal A and B using the single channel and coupled-channels calculations, respectively. **Figure 2.b.** (C, D) shows the distribution at sub-barrier energies, using the single and coupled channels calculations, respectively. The experimental data are taken from ref [17].

4-3. The $^{28}Si+^{150}Nd$ system

In this system, the change of quasi elastic scattering with the angle was studied, depending on the change in the values of the diffusion parameter, and the study was carried out in two cases, in the first case The projectile and target

nuclei were each considered to be inert, single channel (SC) at different values from diffuseness parameter (0.55, 0.63, and 0.71) fm, and 0.63fm was taken to be the standard value. in the second case, we assumed that the projectile nucleus ^{28}Si is rotation coupled to the state 2^+(1.77903 MeV), $E_{4^+}/E_{2^+} = 2.59$ with deformation parameter β_2 = -0.478 where the target nucleus ^{150}Nd was inert**.** The potential depth V_0= 42.2 MeV, the radius parameter r_0 =1.2 fm, and the single phonon state of the quadrupole excitation to the projectile nuclei were employed.

Table 3. The values of the **WS** potential's parameters and χ^2 fitting between experimental and theoretical data for the **^{28}Si+^{150}Nd** reaction

System	Channel	V_0 (MeV)	r_0 (fm)	a_0 (fm)	θ_{cm} ($deg.$)	χ^2	
						σ_{qel}/σ_R	D_{qel}
^{28}Si+^{150}Nd	**SC**	*42.2*	*1.2*	*0.55*	*140*	*0.01936*	*0.03100*
				0.63		*0.05279*	*0.05130*
				0.71		*0.17076*	*0.10976*
	CC	*42.2*	*1.2*	*0.55*	*140*	*0.00843*	*0.00880*
				0.63		*0.00597*	*0.01078*
				0.71		*0.00828*	*0.01623*

In Table (3), According to the results of the χ^2 data, the red line in Fig. 3.a. (A) represents the calculated ratio of the quasi-elastic to the Rutherford cross sections $\left(\frac{d\sigma_{qel}}{d\sigma_R}\right)$, which is 0.01936 at the diffuseness parameter *0.55* fm, V_0 = *42.2* MeV obtained from single channel (SC) data analysis with the projectile ^{28}Si nucleus and target ^{150}Nd nucleus being inert.

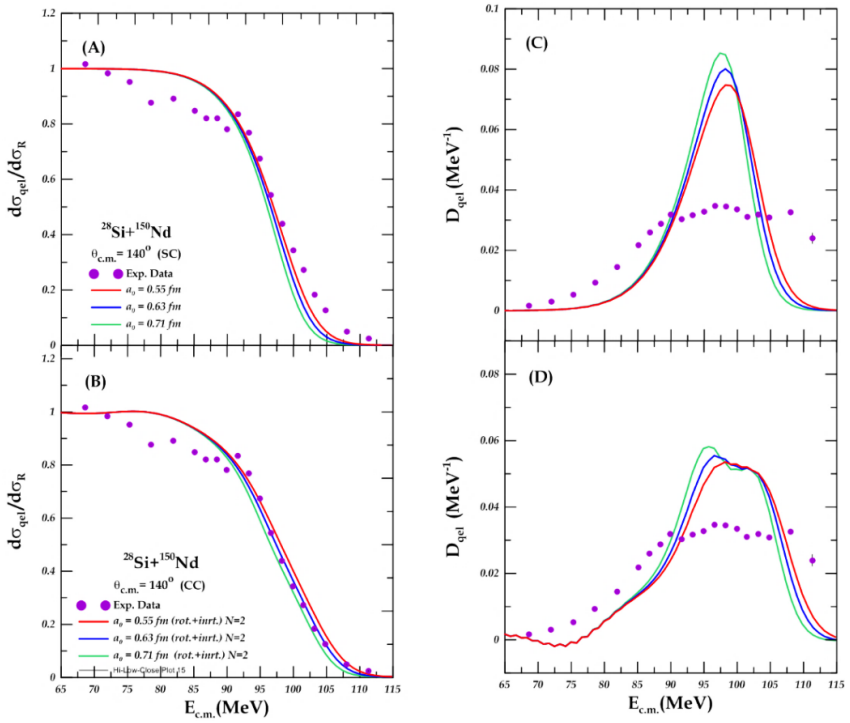

(a) (b)

Figure 3.a. The ratio of the quasi-elastic scattering to the Rutherford cross sections for ^{28}Si+^{150}Nd system at sub-barrier energies. Banal A and B using the single channel and coupled-channels calculations, respectively. **Figure 3.b.** (C, D) shows the distribution at sub-barrier energies, using the single and coupled channels calculations, respectively. The experimental data are taken from ref [18].

It is the curve that is most nearby to the curve of the experimental data. The optimum value for the distribution D is *0.03100*, shown by the hard red line in Fig. 3.b. (C) at the same diffuseness parameter value. According to the coupled-channel calculations with a rotating projectile (P) and inert target (T), it was found that the best value of $\left(\frac{d\sigma_{qel}}{d\sigma_R}\right)$ is *0.00597* at the diffuseness parameter a_0 of *0.63* fm, which is represented by the hard blue line in Fig. 3.b. (B). It is the curve closest to the curve of the experimental data, the best value of the distribution D is *0.00880* at the diffuseness parameter of *0.55* fm denoted by the red-colored curve.

5. CONCLUSIONS

We conclude from this study the following:

1- The standard value of the diffuseness parameter a_0 is not the only one that shows the best match between the theoretical calculations and the practical values, but it is possible to take lower and higher values than the standard value of the diffuseness parameter by 9, and thus we were able to obtain the best match within this range of values.

2- From the calculations of (CC) we notice that it has a significant impact on improving quasi elastic scattering calculations ($\frac{d\sigma_{qel}}{d\sigma_R}$) ,and this was clearly shown on the results of (χ^2) regardless of the value of a_0.

3- We notice in the calculations of (SC) that the theoretical calculations coincide with the practical values at the value of a_0 which is less than the standard diffusion parameter, because the larger the value of the diffuseness parameter, the greater the diffusion of nuclear potential. In addition, the potential barrier in the (SC) is single, while in (CC) calculations it is multiple.

ORCID IDs

Khalid S. Jassim, https://orcid.org/0000-0002-5990-3277

REFERENCES

[1] M. Dasgupta, D.J. Hinde, N. Rowley, and A. M. Stefanini, "Measuring Barriers To Fusion," Annual Review of Nuclear and Particle Science, **48**, 401-461 (1998). https://doi.org/10.1146/annurev.nucl.48.1.401

[2] V.Y. Denisov, "Superheavy element production, nucleus-nucleus potential and μ-catalysis," in AIP Conference Proceedings, **704**(1), 92-101 (2004). https://doi.org/10.1063/1.1737100

[3] L.R. Gasques, M. Evers, D.J. Hinde, M. Dasgupta, P.R.S. Gomes, R.M. Anjos, M.L. Brown, *et al.*, "Systematic study of the nuclear potential through high precision back-angle quasi-elastic scattering measurements," Phys. Rev. C - Nucl. Phys. **76**(2), 024612 (2007). https://doi.org/10.1103/PhysRevC.76.024612

[4] K. Hagino, and N. Rowley, "Large-angle scattering and quasielastic barrier distributions," Phys. Rev. C, 69(5), 054610 (2004). https://doi.org/10.1103/PhysRevC.69.054610

[5] M. Zamrun, K. Hagino, S. Mitsuoka, and H. Ikezoe, "Coupled-channels analyses for large-angle quasi-elastic scattering in massive systems," Phys. Rev. C, **77**(3), 034604 (2008). https://doi.org/10.1103/PhysRevC.77.034604

[6] A.B. Balantekin, and N. Takigawa "Quantum Tunneling in Nuclear Fusion," Rev. Mod. Phys. **70**, 77 (1998). https://doi.org/10.1103/RevModPhys.70.77

[7] K. Hagino, N. Rowley, and A.T. Kruppa, "A program for coupled-channel calculations with all order couplings for heavy-ion fusion reactions," Comput. Phys. Commun. **123**(1-3), 143-152 (1999). https://doi.org/10.1016/S0010-4655(99)00243-X

[8] K. Washiyama, K. Hagino, and M. Dasgupta, "Probing surface diffuseness of nucleus-nucleus potential with quasielastic scattering at deep sub-barrier energies," Phys. Rev. C, **73**, 034607 (2006). https://doi.org/10.1103/PhysRevC.73.034607

[9] K. Hagino, and K. Washiyama, "Probing internucleus potential with large-angle quasi-elastic scattering," AIP Conference Proceedings, **853**, 86-93 (2006). https://doi.org/10.1063/1.2338360

[10] Q.J. Tarbool, K.S. Jassim, and A.A. Abojassim, "Surface diffuseness parameter with quasi-elastic scattering for some heavy-ion systems," Int. J. Nucl. Energy Sci. Technol. **13**(2), 110-119 (2019). https://www.inderscience.com/info/inarticle.php?artid=100758

[11] N.H. Hayef, and K.S. Jassim, "Coupled channels for quasi-elastic scattering of determining diffuseness parameters in Woods-Saxon potential for nuclear reaction," AIP Conference Proceedings, **2414**(1), 030012 (2023). https://doi.org/10.1063/5.0117002

[12] A.J. Hassan, and K.S. Jassim, "Effect of Surface Diffuseness Parameter on Quasi-elastic Scattering Calculations for ^{6}He+^{64}Zn, ^{7}Li+^{64}Zn and ^{8}Li+^{90}Zr Systems," NeuroQuantology, **18**(9), 40-44 (2020). https://doi.org/10.14704/nq.2020.18.9.NQ20214

[13] R.D. Woods, and D.S. Saxon, "Diffuse surface optical model for nucleon-nuclei scattering," Phys. Rev. **95**(2), 577 (1954). https://doi.org/10.1103/PhysRev.95.577

[14] P. Fröbrich, and R. Lipperheide, *Theory of nuclear reactions*, Vol. 18, 1st ed. (Clarendon Press, Oxford Studies, 1996). pp. 18.

[15] M. Dasgupta, D.J. Hinde, J.O. Newton, and K. Hagino, "The nuclear potential in heavy-ion fusion," Prog. Theor. Phys. Suppl. **154**, 209-216 (2004). https://doi.org/10.1143/PTPS.154.209

[16] R.A. Broglia, and A. Winther, *Heavy Ion Reactions: Elastic and inelastic reactions*, (Advanced B. Cummings Publishing Company, 1981).

[17] Y.K. Gupta, B.K. Nayak, U. Garg, K. Hagino, K.B. Howard, N. Sensharma, M. Şenyiğit, *et al.*, "Determination of hexadecapole (β4) deformation of the light-mass nucleus ^{24}Mg using quasi-elastic scattering measurements," Phys. Lett. Sect. B Nucl. Elem. Part. High-Energy Phys. **806**, 135473 (2020). https://doi.org/10.1016/j.physletb.2020.135473

[18] M. Sharma, A. Rani, S. Manda, S. Nath, N. Madhavan, J. Gehlot, Gonika, *et al.*, "Quasi-Elastic Scattering Measurements for ^{28}Si+^{116,120,124}Sn Systems near Coulomb Barrier," Proceedings of the DAE Symp. on Nucl. Phys. **65**, 433-434 (2021). https://inspirehep.net/files/f1ec2021066b5c813665ad770c13244c

[19] S. Biswas, A. Chakraborty, A. Jhingan, D. Arora, B.R. Behera, R. Biswas, N.K. Deb, *et al.*, "Barrier distribution for the ^{28}Si+^{150}Nd system through quasi-elastic excitation function measurement," DAE Symp. Nucl. Phys. **64**, 439-440 (2019). https://inspirehep.net/literature/1803955

ВПЛИВ ПАРАМЕТРУ ДИФУЗНОСТІ НА КВАЗІПРУЖНЕ РОЗСІЮВАННЯ СИСТЕМ ^{25}Mg+^{90}Zr та ^{28}Si+(^{120}Sn, ^{150}Nd) З ВИКОРИСТАННЯМ ПОТЕНЦІАЛУ ВУДА-САКСОНА

Фарах Дж. Хамуд, Халід С. Джасім

Факультет фізики, Освітній коледж чистих наук, Вавилонський університет, Ірак

Було вивчено вплив зміни значень параметра дифузії на розрахунки напівпружного розсіювання (*dσqel*)/*dσR*) і розподілу (D) для одного каналу (SC) і зв'язаного каналу (CC). Три значення були взяті з дифузії для кожного параметра системи. Передбачається, що ядерний потенціал має форму Вудса-Саксона, на яку вказують поверхнева дифузність, глибина потенціалу та параметри радіуса для систем (^{25}Mg +^{90}Zr), (^{28}Si+(^{120}Sn, ^{150}Nd). Хі-квадрат (χ2) застосовується для порівняння найкраще підігнаного значення параметра дифузності між теоретичними розрахунками та експериментальними даними. Згідно з результатами (χ2), ми зазначаємо, що деякі системи досягли гарної відповідності між теоретичними розрахунками та експериментальними даними напівпружнього розсіювання (*dσqel*)/*dσR*) і розрахунками розподілу при стандартному значенні параметра дифузії (a_0=0,63) або при значенні вище або нижче стандартного значення. У випадку (SC) найкраще відповідність було при меншому, ніж стандартне значення параметра дифузії, але у випадку (CC) відповідність була кращою при значенні, вищому за стандартне значення параметра дифузії, оскільки потенційний бар'єр у (SC) одинарний, тоді як у (CC) розрахунки кратні.

Ключові слова: *квазіпружне розсіювання; потенціал Вудса-Саксонса; один канал; сполучені канали; поверхневий параметр дифузності; система важких іонів*